Since January 2020 Elsevier has created a COVID-19 resource centre with free information in English and Mandarin on the novel coronavirus COVID-19. The COVID-19 resource centre is hosted on Elsevier Connect, the company's public news and information website.

Environmental Pollution 272 (2021) 115927

Contents lists available at ScienceDirect

Environmental Pollution

journal homepage: www.elsevier.com/locate/envpol

Ozone pollution mitigation in guangxi (south China) driven by meteorology and anthropogenic emissions during the COVID-19 lockdown☆

Shuang Fu [a], Meixiu Guo [b], Linping Fan [a], Qiyin Deng [c], Deming Han [a], Ye Wei [b], Jinmin Luo [b], Guimei Qin [a], Jinping Cheng [a,*]

[a] School of Environmental Science and Engineering, Shanghai Jiao Tong University, Shanghai, 200240, China
[b] Beihai Ecology and Environment Agency, Beihai, Guangxi, 536000, China
[c] College of Environment, Hohai University, Nanjing, Jiangsu, 210098, China

ARTICLE INFO

Article history:
Received 6 August 2020
Received in revised form
23 October 2020
Accepted 23 October 2020
Available online 27 October 2020

Keywords:
Ozone
COVID-19
Lockdown
South China
CEMS
MLR model

ABSTRACT

With the implementation of COVID-19 restrictions and consequent improvement in air quality due to the nationwide lockdown, ozone (O_3) pollution was generally amplified in China. However, the O_3 levels throughout the Guangxi region of South China showed a clear downward trend during the lockdown. To better understand this unusual phenomenon, we investigated the characteristics of conventional pollutants, the influence of meteorological and anthropogenic factors quantified by a multiple linear regression (MLR) model, and the impact of local sources and long-range transport based on a continuous emission monitoring system (CEMS) and the HYSPLIT model. Results show that in Guangxi, the conventional pollutants generally declined during the COVID-19 lockdown period (January 24 to February 9, 2020) compared with their concentrations during 2016–2019, while O_3 gradually increased during the resumption (10 February to April 2020) and full operation periods (May and June 2020). Focusing on Beihai, a typical Guangxi region city, the correlations between the daily O_3 concentrations and six meteorological parameters (wind speed, visibility, temperature, humidity, precipitation, and atmospheric pressure) and their corresponding regression coefficients indicate that meteorological conditions were generally conducive to O_3 pollution mitigation during the lockdown. A 7.84 μg/m^3 drop in O_3 concentration was driven by meteorology, with other decreases (4.11 μg/m^3) explained by reduced anthropogenic emissions of O_3 precursors. Taken together, the lower NO_2/SO_2 ratios (1.25–2.33) and consistencies between real-time monitored primary emissions and ambient concentrations suggest that, with the closure of small-scale industries, residual industrial emissions have become dominant contributors to local primary pollutants. Backward trajectory cluster analyses show that the slump of O_3 concentrations in Southern Guangxi could be partly attributed to clean air mass transfer (24–58%) from the South China Sea. Overall, the synergistic effects of the COVID-19 lockdown and meteorological factors intensified O_3 reduction in the Guangxi region of South China.

1. Introduction

In response to the COVID-19 (corona virus disease 2019) outbreak, nationwide lockdown measures were implemented by the Chinese central government from the end of January 2020, which brought Chinese society almost to a standstill (Adams, 2020; Bao and Zhang, 2020). The dramatic reduction in human and industrial activity, including vehicle kilometers traveled, industrial operations, construction activities, the operation of restaurants, etc., also contributed to the improved air quality (Bao and Zhang, 2020; Li et al., 2020; Pei et al., 2020; Sun et al., 2020; Yang et al., 2020). Most of these studies analyzed the impact of COVID-19 based on changes in pollutants, including particulate matter (PM) with an aerodynamic diameter < 2.5 μm and 10 μm ($PM_{2.5}$ and PM_{10}), nitrogen dioxide (NO_2), sulfate dioxide (SO_2), carbon

☆ This paper has been recommended for acceptance by Admir C. Targino.

* Corresponding author. 800 Dongchuan Road, Minhang District, Shanghai, 200240, China.
E-mail address: jpcheng@sjtu.edu.cn (J. Cheng).

https://doi.org/10.1016/j.envpol.2020.115927
0269-7491/

monoxide (CO) and ozone (O_3). Specifically, a national decrease in NO_2 concentrations was observed but the SO_2 concentrations remained steady at lower concentrations, despite distinct trends in $PM_{2.5}$ concentrations in different regions. However, there was only a partial improvement in air quality, given the rebound of O_3 concentrations all over China (Li et al., 2020; Pei et al., 2020), which was also observed in other regions of the world, such as Iran (Broomandi et al., 2020), India (Sharma et al., 2020), Brazil (Siciliano et al., 2020) and Europe (Sicard et al., 2020).

Increased tropospheric O_3 concentrations have been a focus of research attention in recent years due to their effect on aggravating respiratory irritation and lung injury, while O_3 has also been linked to short-term memory loss, immune system dysfunction and lymphocyte chromosome abnormality (Wang et al., 2019). Chen et al. (2020) reported an increasing trend in O_3-related mortality with increased O_3 concentrations from 2014 to 2018. Considering that the cellular receptors in the lungs are the main target of COVID-19, and are vulnerable to attachment by the virus spikes (Ali and Alharbi, 2020), the chances of infection could increase in subjects exposed to severe air pollution. Zhang et al. (2020b) suggested a relationship between higher concentrations of air pollutants (increased O_3 and $PM_{2.5}$ in particular) and increased risk of COVID-19 infection. The high concentrations of atmospheric oxidant pollutants may increase the susceptibility of the population to respiratory complications due to COVID-19 (Babu et al., 2020). Besides human health, high O_3 concentrations also have adverse effects on ecosystem productivity (Monks et al., 2015). Amplified O_3 pollution under the lockdown has become a concern beneath the benign surface of air quality improvement (Zhang et al., 2020b). It should be made clear that in our observation, with the national and even global trends of O_3 increasing during the COVID-19 lockdown period, there were some regions where O_3 concentrations did not increase or even significantly decreased.

Besides the strong sensitivity to meteorological changes in physical and chemical processes (Chen et al., 2020; Zhang et al., 2018), O_3 air quality can be largely affected by anthropogenic emissions. The COVID-19 restrictions contributed to reduced anthropogenic activities, thereby providing unique opportunities for atmospheric research. In this study, we attempted to distinguish between the contributions of emission controls and variability in meteorological factors to the reduced O_3 concentrations in the South China region. This study will provide reference for a comprehensive assessment of the impact of lockdown responses.

An integrated measurement-emission-modelling approach has been adopted in this study that includes observations of the AQI and ambient pollutants. Our quantitative analysis uses a developed multiple linear regression (MLR) model, and our impact analysis of key source emissions and long-range transport is based on the continuous emission monitoring system (CEMS) and HYSPLIT model, respectively. This study aims to (1) study the variations of conventional air pollutants under the different response levels in the Guangxi region, (2) quantify the driving force of declined O_3 concentrations during the lockdown period, and (3) to comprehensively assess the influence of local residual sources and long-range transport on regional air quality. It is expected that these results may provide a reference for the mitigation of O_3 pollution through O_3 characterizations and identifying the driving factors of O_3 reduction in a typical region of South China.

2. Data and methodology

2.1. Study domain and time

In this study, our research domain covers the entire Guangxi region of South China, including fourteen prefecture-level Chinese cites and 50 monitoring sites (Fig. 1). The city of Beihai is representative of general underdeveloped areas in Guangxi, in South China, with long-term dominant industrial structure as the primary industry (Liu et al., 2019). Detailed investigations focused on Beihai, a city with a population of 1.68 million living in an area of 3337 km^2 (in 2018). The investigations were conducted to reflect the causes of air quality changes during the lockdown period in the Guangxi region.

The six-month period in 2020 during which COVID-19 restrictions were imposed in the Guangxi region were divided into three stages based on the response levels: Pre-lockdown, Level I response, and Level III response. Some industries resumed operation as of February 10, 2020, and by the end of April, society had mostly returned to normal. To better understand the details of the air quality changes, combined with human activities, Level I response was subdivided into three periods: (i) Spring Festival; (ii) Level I lockdown; and (iii) Level I restoration (from February 10). Level III response was subdivided into (i) Level III recovery (February 25 to April 30); and (ii) Level III operation (May and June). Following two stages of gradual social resumption (i.e. Level I restoration and Level III recovery), the Level III operation was classified into the full operation phase. For year-by-year comparisons, the period 2016–2019 was classified accordingly, as shown in Table S1. Considering the temporal variations of multiple factors (population movements, industrial operations, government controls, meteorological conditions, etc.), apart from a separate two-day period during the Lunar New Year, other stage divisions in this study are made according to the Gregorian calendar, the details of which are described in Supplementary Text 1.

2.2. Data sources

The hourly ambient mass concentrations of criteria air pollutants including $PM_{2.5}$, PM_{10}, NO_2, SO_2, CO, and O_3 were measured at 50 sites in fourteen cities during the first half years of 2016–2020, which were acquired from real-time data released by the air monitoring data center of the Ministry of Ecology and Environment of the People's Republic of China (MEE, 2020). To generate continuous grid concentration data in the Guangxi area, the inverse distance weighting (IDW) method was used to interpolate the concentrations measured at sampling sites (Chen et al., 2020; Shen et al., 2017). Hourly nitric oxide (NO) and NOx ($NO + NO_2$) concentrations were obtained from the Beihai Air Quality Network Monitoring and Management Platform (Beihai-AQM, 2020) and used as supplementary data for this analysis. The meteorological data on urban precipitation and wind speed and direction were retrieved from the European Centre for Medium-Range Weather Forecasts Reanalysis Interim data (ERA-Interim, 2020), which had a temporal resolution of 3 h. In additional, hourly meteorological parameters at different monitoring sites including wind speed, temperature, relative humidity (RH), atmospheric pressure, and visibility (at daily resolution), were obtained from Beihai-AQM. All data were manually inspected during processing. Following the method adopted by Shu et al. (2017) and Zhu et al. (2019), invalid and missing data have been collated. Moreover, meteorological parameters and pollutant concentrations were matched at temporal and spatial scales to establish association among variables.

The real-time monitoring data of key industrial emission sources in Beihai (including hourly dust, NOx, and SO_2 emissions) was obtained from the continuous emission monitoring system (CEMS, 2020). A comparative analysis was carried out on the online monitoring data of 48 smoke outlets from 16 key industries over 2 years (2019–2020), including the COVID-19 lockdown period (Table S2).

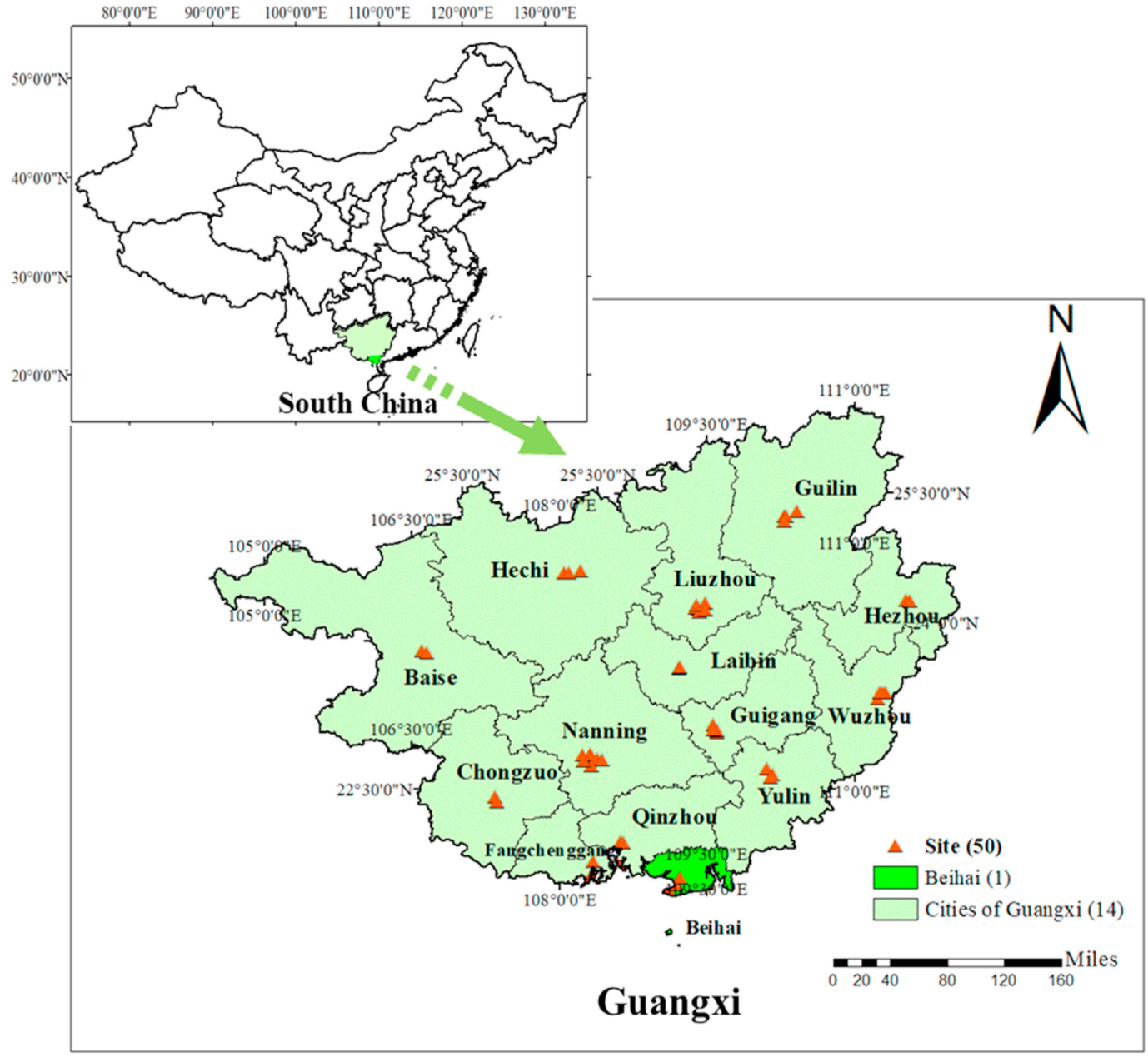

Fig. 1. The study area and observational locations in the study.

2.3. Multiple linear regression model

An MLR model establishes a functional relationship between a response variable and several explanatory variables, and such models have been successfully applied to study $PM_{2.5}$ and O_3 variations driven by meteorological variations (Chen et al., 2020; Zhai et al., 2019; Zhao et al., 2020). In view of the short time interval (i.e. the Level I lockdown period, 15 days) and lack of fluctuations in non-meteorological factors (constant anthropogenic influences) in previous years (2016–2019), the stepwise multiple linear regression (MLR) model used by Zhai et al. (2019) to eliminate confusion due to seasonal variations and long-term trends, was not applicable to this study. We therefore developed an MLR model, based on 5-year data from different monitoring sites, to quantify the effect of meteorology on O_3 variability during the Level I lockdown period (January 26 to February 9, 2020), using Eqs. (1) and (2). Based on the MLR inverse calculation, the meteorology-driven O_3 anomalies in 2020 compared with previous years, are estimated by $\Delta C_{Ms}(t)$. The residual, after removing the meteorological influence from the MLR results, is given by Eq. (3), which we attributed to anthropogenic influences, $\Delta C_{As}(t)$.

$$C_{0s}(t) = \sum_{k=1}^{n} \beta_{k,s} \times Met_{0\ k,s}(t) + b_s + \varepsilon \quad (1)$$

$$\Delta C_{Ms}(t) = \sum_{k=1}^{n} \beta_{k,s} \times Met_{\ k,s}(t) + b_s + \varepsilon - C_{0s}(t) \quad (2)$$

$$\Delta C_{As}(t) = C_s(t) - [\sum_{k=1}^{n} \beta_{k,s} \times Met_{k,s}(t) + b_s + \varepsilon] \quad (3)$$

where $C_{0s}(t)$ and $C_s(t)$, respectively, are the observed daily concentrations of O_3 for observation site s in 2016–2019 and 2020, $Met_{0\ k,s}(t)$and $Met_{k,s}(t)$ are, respectively, the daily values of the kth meteorological variable for observation site s in 2016–2019 and 2020, $\beta_{k,s}$, b_s, and $\varepsilon$are the regression coefficient, intercept and deviation, respectively, fitted over the period used in the MLR model, and $\Delta C_{Ms}(t)$and $\Delta C_{As}(t)$are the expected variations in O_3 concentration driven by meteorological variability and anthropogenic influences, respectively.

Five meteorological variables [pressure, temperature, relative humidity, wind speed (WDS) and precipitation] were entered into the MLR model. Unlike previous studies (Chen et al., 2020; Zhai et al., 2019), the meteorological variables used in the MLR model were normalized separately, based on Min-Max Normalization (MMN), to improve their effectiveness. Dimensionless parametrization was carried out such that the variations in the meteorological variables, and the corresponding regression coefficients, were comprehensible and comparable. Outliers (more than three standard deviations [3SD]) were removed through case diagnostics, and the MLR model was re-run to improve reliability of the input samples. In addition, upon examination, the meteorological parameters in the MLR inverse calculation were included in the variation ranges of the input samples, thereby slightly improving the reliability of the MLR prediction.

2.4. Backward trajectory cluster analyses

To study the regional transport of air masses in the Guangxi area, the HYSPLIT model (Version 5.0), developed by NOAA ARL, was used to compute the backward trajectories with meteorological inputs from the NCEP/GDAS data sets at a 2-h temporal resolution. The backward trajectories of air masses during a 36-h period were computed at a height of 500 m above ground level in eight Guangxi surrounding cities, beginning at 00:00 a.m. (local time) every day during the lockdown periods. Subsequently, the HYSPLIT model was applied to the cluster analyses based on the sub-sets of backward trajectories (Hong et al., 2019; Rolph et al., 2017).

3. Results and discussion

3.1. Air quality before and during the COVID-19 periods

The average air quality index (AQI) for Guangxi in the first half of 2020 was 46.27, down 10.1% compared with that in 2016–2019. Fig. 2 and S1 show the levels and changes in air quality before the COVID-19 lockdown and during the Level I–III response periods. Compared with previous years, a pronounced improvement of air quality was observed throughout the Guangxi region during the lockdown period. Under the dual advantage of regular Spring Festival emission reductions and COVID-19 lockdown, AQI declined dramatically with a reduction of 75.3% ± 8.1% (mean ± SD) during the Spring Festival, which was more significant than the decrease during the Level I lockdown period (37.3% ± 8.1%). In contrast, during the relatively relaxed Level III response period, the AQI only decreased slightly and even showed an upward trend during the Level III operation period. The AQI bounced back partially after lockdown in Guangxi, but it was still lower than before (Fig. S1) due to the regular COVID-19 control and prevention measurements (Yang et al., 2020).

Overall, there was a decline in conventional air pollutants throughout almost the entire Guangxi region as a consequence of lockdown, compared with previous years. During the Level I response period, concentrations of $PM_{2.5}$, PM_{10} and SO_2 plunged, especially while Guangxi was in lockdown; the average reduction of NO_2 concentrations was 37.8% relative to that in 2019, and consistent with the national mean reduction of 35.7% in NO_2 concentrations (Zheng et al., 2020). Among the 14 investigated cities, there were some differences in the changes of CO concentrations, which ranged from −47.6% to 23.4%. The O_3 reductions in the 14 investigated cities were considerable during the Spring Festival (43.7% ± 10.6%) and Level I lockdown (14.5% ± 11.6%) periods, with a slight rebound during the Level I restoration period (9.7% ± 16.6%). Unlike in the rest of China and elsewhere in the world (Li et al., 2020; Sharma et al., 2020; Sicard et al., 2020; Siciliano et al., 2020; Zheng et al., 2020), amplified ozone pollution was not observed in the Guangxi region during the COVID-19 lockdown period. During the Level III response period, with routine human activities gradually resuming operation, the mean changes of $PM_{2.5}$, PM_{10}, NO_2, SO_2, CO, and O_3 in the Guangxi region for the recovery (full operation) period compared with the same period in 2016–2019 were −25.5% (−12.6%), −22.6% (−5.9%), −11.4% (−1.2%), −26.9% (−22.5%), −18.6% (−20.8%), and −4.9% (10.3%), respectively, showing that the Level III responses also contributed to the air quality improvements. In terms of the spatial distribution of air pollutants during post-lockdown, O_3 and NOx showed opposite trends (Fig. 2). In particular, during the Level I restoration and full operation phases, increased O_3 was always accompanied by decreased NO_2.

Air quality changes also varied among these prefecture-level cities. In addition to the different meteorological conditions and response measures, the variations were also related to the spatial distribution of industrial activities in the regions. For example, power plants are mainly distributed in western and central Guangxi, while steel plants and petrochemical industries are concentrated in northern and southern Guangxi, respectively (Liu et al., 2019). As a typical coastal city of Southern Guangxi, air quality changes in Beihai city during the COVID-19 response reflect the average conditions in the Guangxi region (Fig. 2). As detailed below, the atmospheric characteristics and year-to-year changes were investigated, based on the data collected in Beihai. Figure S3 shows the daily mean concentrations of criteria air pollutants in Beihai during different periods over the past 5 years. The daily mean concentrations of the six criteria pollutants ($PM_{2.5}$, PM_{10}, NO_2, SO_2 CO and O_3) were at their lowest under the lockdown (32.18, 41.66, 9.74, 7.55, 0.78 × 10^3, 58.38 μg/m^3) relative to corresponding periods in the previous 5 years, and compared to the 2019 measurements, their concentrations decreased by 30.1%, 32.8%, 34.7%, 14.2%, 14.5% and 37.0%, respectively. A sharp reduction in NO_2 and a significant decrease in O_3 were observed, with concentrations of 24.4% and 58.4% of the air quality standard limits, respectively. Moreover, the long-term upward trend of O_3 concentrations in previous years was reversed during the Level I lockdown period, indicating that the driving force of ozone decline was significant in 2020. Additionally, SO_2 was maintained at a low concentration of 6.09–8.30 μg/m^3 under the lockdown, suggesting a significant decrease in SO_2 emissions (especially coal consumption) (Qu et al., 2016; Zheng et al., 2018). During the phase of gradual resumption of social activity (i.e. Level I restoration and Level III recovery), SO_2 (O_3) concentrations increased by 17.6% (15.6%) compared with those in 2019; while NO_2 (CO) concentrations still declined by 12.3% (28.3%); PM_{10} ($PM_{2.5}$) concentrations declined slightly, with an average decline of 1.7% (1.8%). CO and $PM_{2.5}$ concentrations decreased to their lowest values during the full operation period (Fig. S2), consistent with their temporal distribution over the Yangtze River Delta Region (YRD) by Li et al.

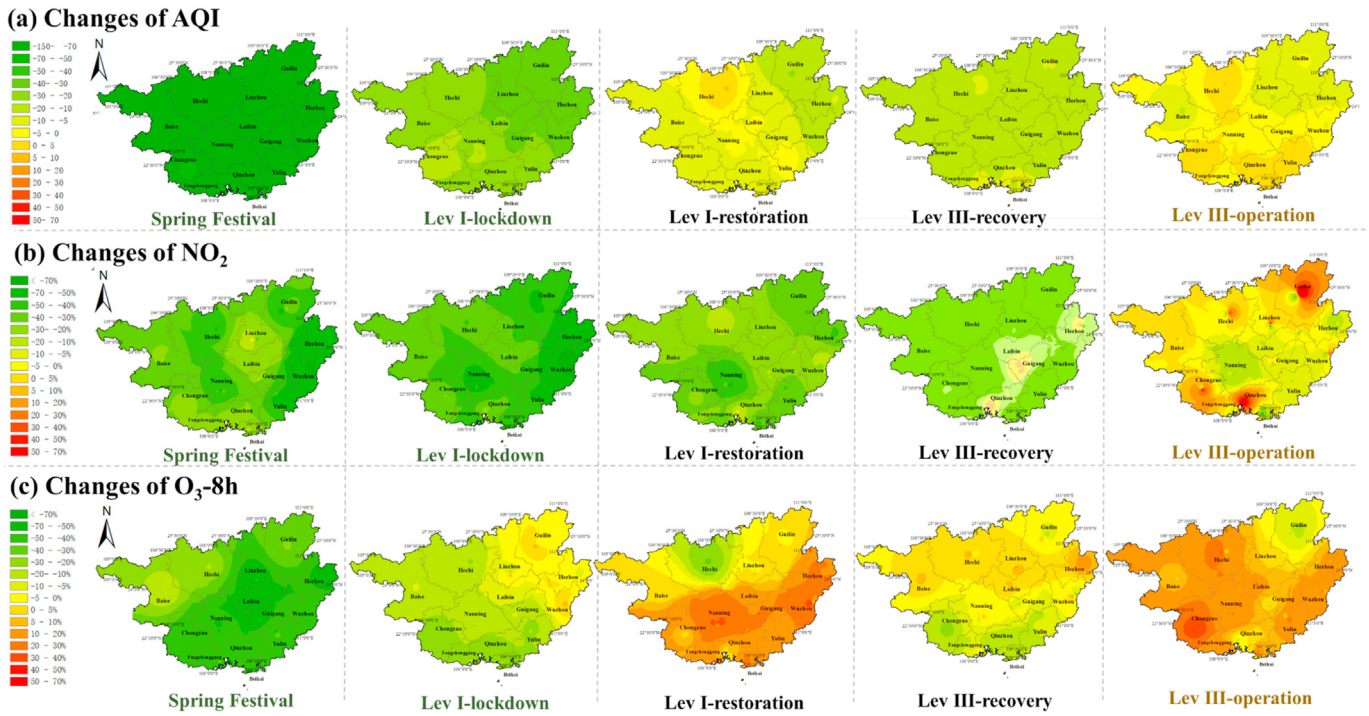

Fig. 2. Changes of AQI (a) and air pollutants [NO_2 (b) and O_3-8h (c)] during the corresponding COVID-19 response periods in 2020 compared with the same period 2016–2019 in the Guangxi region.

(2020), indicating that reductions in their concentrations were more dependent on a longer-term response. Concentrations of other conventional pollutants (except for O_3) declined slightly during the full operation period compared with previous years, similar to the changes preceding the COVID-19 epidemic outbreak.

3.2. Characteristics of atmospheric pollutants during the COVID-19 lockdown period

As shown in Fig. 3, S3, and S4, the diurnal variations and time series of the atmospheric pollutants, as well as their correlations under both hourly and daily resolutions, were investigated to analyze their characteristics during the lockdown period. In general, despite weaker peaks of all conventional pollutants during the lockdown period, the diurnal trends of generation and consumption of pollutants were consistent with those in previous years (Fig. S4). There was a general decline in the hourly $PM_{2.5}$ concentration, indicating reduced anthropogenic emissions from fossil fuel combustion and biomass burning (Zhang and Cao, 2015). The slightly increased $PM_{2.5}/PM_{10}$ ratio indicated the meteorological conditions were conducive to deposition of coarser particles. NO_2 showed weaker bimodal trends consistent with morning and evening traffic peaks, and the observed NO_2 reductions were linked to the lockdown and the subsequent changes in industrial and traffic activity (Kuerban et al., 2020). Additionally, during the lockdown period, the evening NO_2 peak was more pronounced than the morning peak. The correlations between the hourly NO_2, SO_2 and CO concentrations were significantly positive (Fig. 3), suggesting that their emission sources were highly consistent. Moreover, as shown in Fig. S4, both the SO_2 and NO_2 concentrations decreased owing to reduced anthropogenic emissions, and the NO_2/SO_2 ratio was lower than that in 2019, especially during the evening rush hour. Given the lower ratio of NOx to SOx from coal combustion (1:2) instead of combustion of vehicle fuels (8:1–13:1), it was assumed that, during the lockdown period, the low NO_2/SO_2 ratio (1.25–2.33) showed that automobile exhausts contributed little to air pollution (Tang et al., 2013; Zhang et al., 2020a). The investigation of night-time light by Liu et al. (2020) also revealed that the reduction of non-essential industries and motor vehicle usage during the COVID-19 lockdown has had a crucial impact on improved air quality.

The hourly $PM_{2.5}/CO$ ratio, a good tracer of primary combustion sources, is also shown in Fig. S4. The diurnal distributions showed a less pronounced $PM_{2.5}/CO$ ratio peak in the daytime, indicating secondary formations from the photochemical reaction were relatively weak (Zhang and Cao, 2015). Enhanced overnight $PM_{2.5}/CO$ ratios were observed during the lockdown period, with its high values lagging behind the high NO_2 emissions by ~2 h, suggesting that NO_2 emitted from coal combustion contributed to the primary emissions and secondary production of $PM_{2.5}$. The time series in Fig. S3 showed that high values of primary pollutants (especially NOx, SO_2) and $PM_{2.5}$ were observed less and were more likely to occur at midnight than in 2019, which was presumably due to the staggered daytime activities of the population under the COVID-19 lockdown restrictions.

As shown in Fig. S4, a lower unimodal tendency was observed for O_3. Comparisons of diurnal variations of O_3 during different periods showed its lowest concentration at 16:00 and slightly higher values overnight, indicating the weaker photochemical formation and consumption under lockdown, whereas the variations of O_3 still conformed to the normal diurnal fluctuations (Hui et al., 2019; Liao et al., 2017). Given that the daily emissions of NO were relatively lower and that it is easily oxidized into NO_2 during the daytime, the diurnal NO/NO_2 ratios were slightly lower. In the afternoon (12:00–17:00), during the lockdown period, the higher NO/O_3 ratios indicated that the titration effect of NO in the NOx cycle was considerable in photochemical reactions. Additionally, as shown in Fig. 3, comparative correlations of hourly and daily resolutions during the lockdown periods in 2020 and the period 2016–2019, showed that O_3 was always significantly negatively

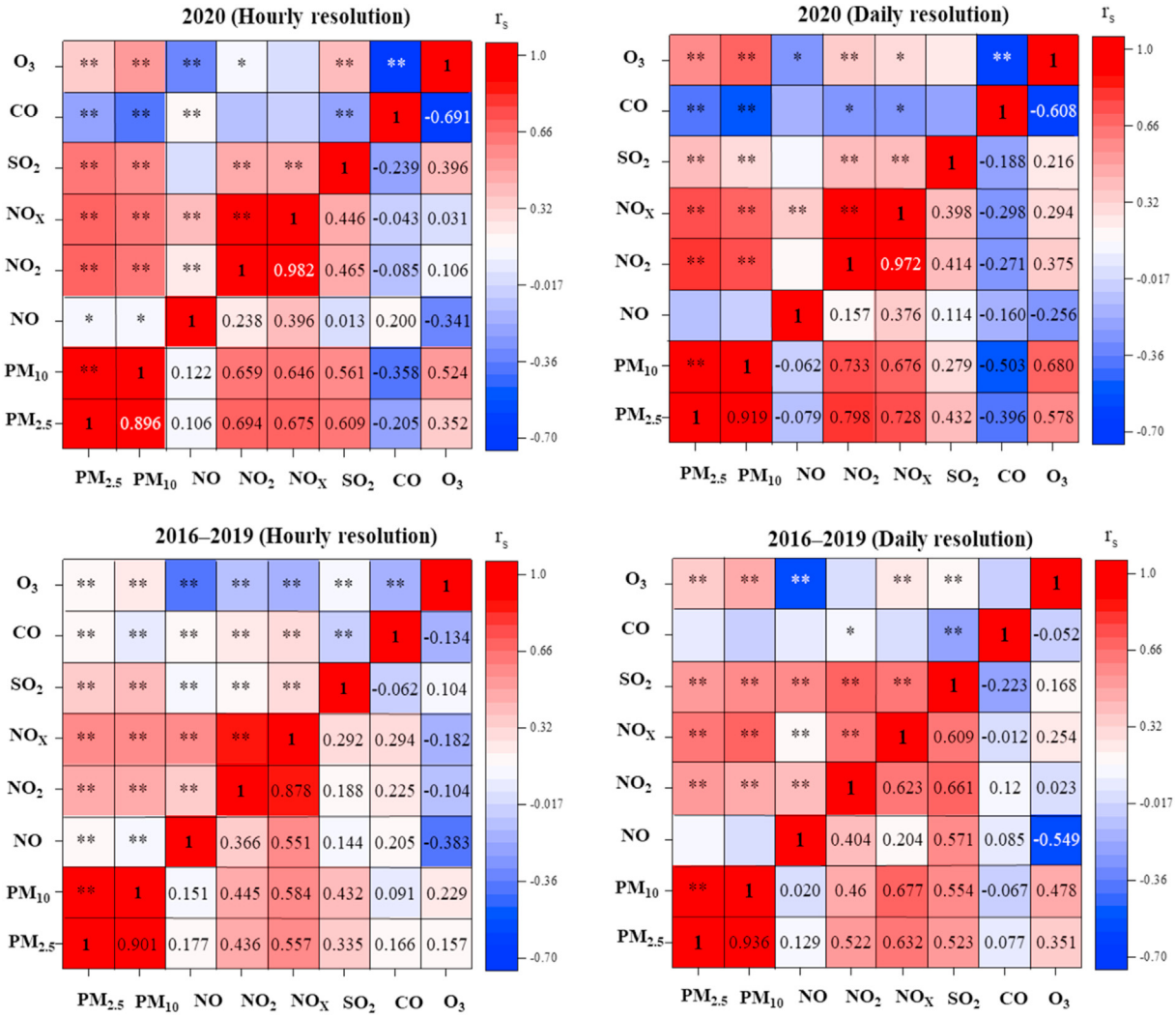

Fig. 3. Correlations between air pollutants based on hourly and daily resolutions during lockdown periods (*$p < 0.05$; **$p < 0.01$).

correlated with NO. In previous years (2016–2019), the significant positive correlation with NO_2 in daily resolution, instead of negative correlations in hourly, showed that increased O_3 concentrations are highly associated with increased daily emissions of O_3 precursors. During the lockdown period in 2020, O_3 showed a strong positive correlation with NO_2 in daily resolution ($r_s = 0.375$, $p < 0.01$), and a moderate positive correlation in hourly resolution ($r_s = 0.106$, $p < 0.05$), indicating, unlike previous studies (Fu et al., 2020), that O_3 concentrations were more likely to depend on NOx concentrations. Besides variabilities in its precursors, as a secondary photochemical pollutant, fluctuations in O_3 concentrations can also be driven by changes in meteorological conditions, which will be detailed below.

3.3. Variations in meteorological parameters and their correlations with O_3

The general meteorological conditions of Beihai during the first six months of 2020 were the mild temperature (8.75–35.2 °C), modest atmospheric pressure (995.60–1006.35 Hpa), and variable RH (37.5–100%) and wind speed (0.10–9.60 m/s) with a heavy total precipitation (1256.40 mm). The hourly temperature was significantly negatively correlated with RH ($r_s = -0.188$, $p < 0.01$) and atmospheric pressure ($r_s = -0.826$, $p < 0.01$). Compared to the previous 4 years, the daily mean O_3 concentrations during the corresponding lockdown stages were significantly negatively correlated with RH ($r_s = -0.211$, $p < 0.01$), wind speed ($r_s = -0.162$, $p < 0.01$) and precipitation ($r_s = -0.227$, $p < 0.01$), and strongly positively correlated with temperature ($r_s = 0.377$, $p < 0.01$) and atmospheric pressure ($r_s = 0.155$, $p < 0.05$). A moderate negative correlation with visibility ($r_s = -0.015$) was also observed.

Compared to previous years, the temperature during the lockdown period in 2020 was relatively lower (Fig. S3). The daily mean temperature was 0.67 °C lower than that during the period 2016–2019, and the average daytime (8:00–17:00 local time) temperature with a mean of 16.05 °C (SD: 3.92 °C) was 6.17 °C lower than that in 2019, which was unfavorable for the photochemical formation of O_3 and biogenic emissions of O_3 precursors (Liu and Wang, 2020). Compared with previous years, the increased RH (+5.5%) was accompanied by increased cloud fraction and more precipitation (+54.4%), which facilitated the deposition of pollutants, but restricted the formation of photochemical products (Hui et al., 2018). Synchronous faster wind speed (2.12 ± 1.13 m/s) and improved visibility (18.21 ± 9.61 km) can promote the diffusion and dilution of pollutants, as well as a reduction in O_3 concentrations. Although visibility was insignificantly correlated with O_3, the covariation between visibility and wind speed ($r_s = 0.215$, $p < 0.01$) was reflected. As shown in Fig. S3, on January 25, 2020, the O_3

(21.10 μg/m^3) and $PM_{2.5}$ (6.50 μg/m^3) concentrations reached their lowest values at 9:00–13:00 and 23:00, respectively, synchronous with the low daily temperature (18.81 °C), high humidity (93.24%), heavy precipitation (63 mm/d), higher wind speed (2.75 m/s) and moderate pressure (1012.16 Hpa). However, during the lockdown period, short-term maximum values of O_3 were also observed, in particular on 31 January and February 6, 2020, with previously high concentrations of O_3 precursor (NO_X) and favorable photochemical conditions.

3.4. O_3 concentration determination using driven variations in the MLR model

To quantify meteorological influences on O_3 trends during the Level I lockdown period, we developed an MLR model to determine the relationships between O_3 concentrations and significantly correlated meteorological variables (excluding visibility), based on synthetic data from the previous 4 years. The six meteorological variables (daily atmospheric pressure, temperature, RH, WDS and precipitation) measured at different sites, were normalized separately based on MMN, and the dimensionless parametrization was carried out such that the variables were comprehensible and comparable. Comparison of MMN variables showed that atmospheric pressure (−0.10) and RH (+0.06) varied from previous years, followed by WDS (+0.05), temperature (−0.05) and precipitation (−0.01). The regression coefficients in MLR model output showed that the changes in O_3 concentration were most affected by temperature (+72.03) and RH (−45.01), followed by precipitation (−28.96), atmospheric pressure (+26.28) and WDS (−15.20). By assuming no fluctuations in non-meteorological factors (i.e. constant anthropogenic influences), the O_3 concentrations affected by meteorological influences during this lockdown period were mainly distributed in the range of 60–100 μg/m^3, with a mean of 79.81 μg/m^3. To best exhibit the O_3 concentration distributions under the influence of multiple factors, as shown in Fig. 4, the RH, precipitation, pressure, and WDS were renormalized and then integrated into the phase diagrams, given their positive correlations in daily resolution. The pronounced O_3 pollution was always accompanied by synchronous high temperature, low RH and precipitation, with weak pressure and WDS. Change in these meteorological variables consistently drove the mean O_3 concentration down (total decrease 7.84 μg/m^3) by RH (29.5% change), pressure (29.5% change), temperature (37.8% change), and WDS (7.9% change), while the potential elevated effect (up to 4.7%) was due to precipitation changes. During the Level I lockdown phase, the mean O_3 concentration decreased by 34.2%, based on the previous 4-year baseline (87.65 μg/m^3). However, as shown in the yellow zone in Fig. 4(c), the rising O_3 concentrations driven by meteorological factors were evident in the first half of this period. According to the MLR estimation, other decreases (4.11 μg/m^3) due to non-meteorological variations, were attributed to reduced anthropogenic emissions of O_3 precursors, accounting for 34.4% of the observed O_3 decreases. This showed that, under the implementation of lockdown restrictions, variations in anthropogenic emissions had a considerable effect on the mitigation of ambient O_3 concentrations.

3.5. Impact of industrial emissions on the variation in pollutants during the COVID-19 lockdown

Based on the real-time monitoring of 48 smoke outlets from CEMS in 16 enterprises, variations in key industrial emissions were analyzed to better understand the impact of industrial activities on changes in air quality during the COVID-19 lockdown period. As shown in Fig. 5, compared with the same periods in 2019, the total dust (44.8%) and NOx (34.3%) emissions declined significantly, while little variation was observed in SO_2 emissions (−2.8%). Combined with Fig. 5 and S4, the mean diurnal variations in dust, SO_2 and NOx emissions showed consistency with those of ambient pollutants measured by Beihai-AQM during the COVID-19 lockdown, in contrast with the inconsistencies of those in 2019, thus confirming that emissions from residual enterprises were significant contributors to primary pollutants present during lockdown. Power plants, petrochemical industries and cardboard processing plants did not show significant reduction in activity during the COVID-19 lockdown period, and even increased activity, while the emissions from iron and steel plants, non-metallic mineral manufacturing and refined sugar plants fell dramatically. Given the closure of other small-scale industries and dramatic reduction in mobile source activities, with the decrease in ambient NOx concentrations and slight decrease in the emission of volatile organic compounds (VOCs) (Li et al., 2020; Siciliano et al., 2020), the VOCs/NOx ratio was likely to be higher than during the same period in 2019.

Siciliano et al. (2020) reported that, under VOC-controlled conditions, the increase in O_3 concentrations during the lockdown period in their research region could be attributed to the significant increase in NMHC/NOx ratios. With the VOC-limited regimes in most regions of China (Wang et al., 2017), the national increase in O_3 could be linked to the decreased NOx, in addition to the increased VOCs/NOx ratio. On the contrary, in Beihai—classified as a transitional regime (VOCs/NOx ~ 8:1) based on the 2018 measurements (Fu et al., 2020), the VOCs/NOx ratio was expected to greatly exceed the transitional threshold from double-controlled regime to NOx-limited (VOCs/NOx > 12) under the lockdown. Based on the assumption, the drop in NOx concentrations contributed to the decline in O_3 concentrations in this region of South China. This case also confirmed the significant positive correlation with NOx and can be linked to the MLR results, suggesting that changes in local anthropogenic emissions during the lockdown period would have pushed the transformation of O_3 formation regime. O_3 concentrations under transitional regimes are sensitive to both VOC and NOx variations. For the spatial distribution of air pollutants following the lockdown response (shown in Fig. 2), the increased O_3 was always accompanied by decreased NO_2, especially when there was a significant increase in O_3 concentrations (Level I restoration period in the resumption and full operation phases). The apparent negative correlation during these periods suggested that, after the lifting of lockdown restrictions, the system likely reverted to the VOC-limited regime.

3.6. Effect of regional transmission based on backward trajectory analyses

Given that long-range transport is an important factor in regional variations in O_3 concentrations (Sun et al., 2016; Zhang et al., 2016), a cluster analysis of back trajectories in the surrounding Guangxi cities was carried out to analyze the air mass transport patterns during the COVID-19 lockdown period. As shown in Fig. S5, in addition to the influence of adjacent areas, air masses reaching Southern Guangxi also originated from the South China Sea, and advected along the coast. In particular, Beihai was most frequently affected by onshore air masses (Clusters 1 and 2, 58%), followed by Chongzuo (Clusters 1 and 3, 45%), Yulin (Clusters 1 and 3, 31%) and Nanning (Cluster 3, 24%). In view of the clean air from the South China Sea (Fu et al., 2020) and lower O_3 concentrations in Southern Guangxi cities (Fig. S1), we could conclude that the regional transport of air masses facilitated the overall decline in O_3 in Southern Guangxi. The air masses affecting Northern Guangxi (including cities such as Henzhou, Guilin and Hechi), however,

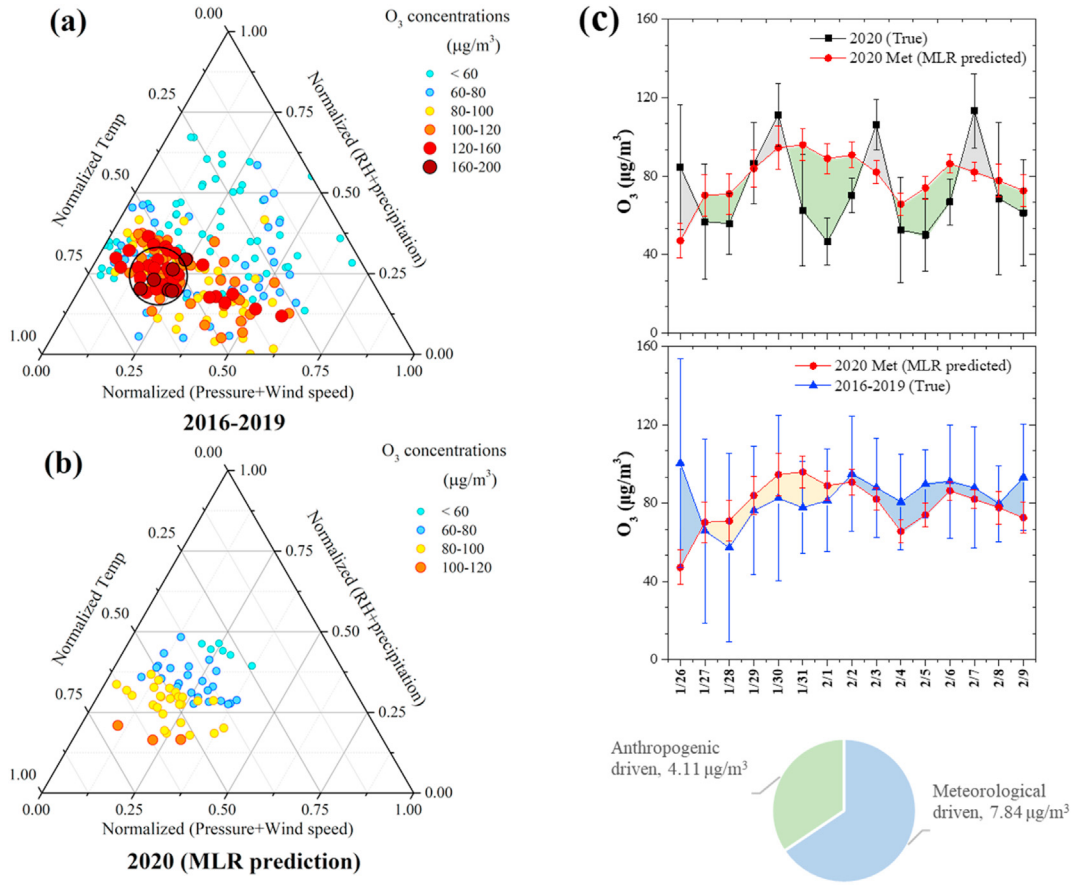

Fig. 4. The distribution of O_3 concentrations dominated by normalized meteorological parameters in previous years (a) and in 2020 (b), as well as predicted daily concentrations and overall decline in O_3 levels driven by anthropogenic and meteorological variations [c, anthropogenic driven: the declined (elevated) levels shown in the green (gray) zone; and meteorologically driven: the declined (elevated) levels shown in blue (yellow) zone) during the lockdown period, using the MLR model. (For interpretation of the references to colour in this figure legend, the reader is referred to the Web version of this article.)

mainly came from Central China. Northerly and easterly air flow from Central China dominated the air mass transport to Ginlin (Clusters 1 and 3, 65%) where a slightly elevated local O_3 phenomenon was observed, which could be linked to the high O_3 values observed in Central China (Pei et al., 2020; Sicard et al., 2020; Sun et al., 2016). The air mass reaching Hezhou and Yulin (Eastern Guangxi) was mainly influenced by local sources based on the regional transport from surrounding areas, shown in the Clusters 1 (22%) and 3 (37%) for Hezhou, and Cluster 2 (69%) for Yulin. In comparison, besides the nearby transport patterns in Western Guangxi, as observed in Baise (Clusters 1 and 2, 87%), Hechi (Clusters 1 and 4, 59%), Chongzuo (Cluster 3, 50%) and Nanning (Cluster 2, 35%), the long-range transport patterns from the inland area were similar (3–5%). In general, given the low ozone concentrations observed in the entire Guangxi area during the COVID-19 lockdown period, more internal transmission would not aggravate O_3 pollution. Northern Guangxi was affected by the air masses with high O_3 concentrations from Central China, especially in Guilin; while the decline in O_3 concentrations was more obvious in the southern coastal area, partly attributed to the effects of clean air flow from the South China Sea.

4. Conclusions

In general, an improvement in air quality with an overall decline in conventional pollutants was observed throughout the Guangxi region as a consequence of the COVID-19 lockdown. Interestingly, the reduction of O_3 in the Guangxi region differed from the national trend of amplified ozone pollution. Focusing on the decreasing O_3 concentration in this region, we analyzed the meteorological variability and the influence of human activity under lockdown. Both the Pearson's correlations and corresponding regression coefficients between the daily O_3 concentrations and meteorological parameters show that the pronounced O_3 pollution was always accompanied by high temperature, low RH and precipitation, as well as low pressure, weak WDS and visibility. Compared to previous years, the meteorological conditions during the lockdown period in 2020 (such as higher RHs, lower temperatures, and weaker pressures) were generally conducive to O_3 depletion. According to the MLR model, synergistic effects of the lockdown (34.4%) and meteorology (65.6%) intensified the decrease in O_3 concentrations in the entire region.

Furthermore, significant correlations between hourly primary atmospheric pollutants and their consistency with hourly pollutant emissions monitored by CEMS reflected changes in the structure of anthropogenic sources during the lockdown period. Also, it was likely that the O_3 formation regime transformed to NOx-limited. Thus, the decrease in NOx contributed to the decreased O_3 concentrations in the Guangxi region. Combined with regional transmission in Guangxi, it was concluded that favorable meteorological conditions, reduced local emissions and small exogenous transmission of O_3 precursors under the lockdown conditions resulted in low ozone concentrations in the Guangxi region.

Fig. 5. Emission variations of dust, SO_2, and NOx observed by CEMS during lockdown period.

Author statement

Shuang Fu: Methodology, Formal analysis, Investigation, Writing - original draft, Visualization, Jinping Cheng: Conceptualization, Methodology, Supervision, Meixiu Guo: Investigation, Resources, Project administration, Linping Fan: Resources, Investigation, Qiyin Deng: Resources, Investigation, Deming Han: Investigation, Writing- Reviewing and Editing, Ye Wei: Investigation, Resources, Project administration, Jinmin Luo: Investigation, Resources, Project administration, Guimei Qin: Investigation.

Declaration of competing interest

The authors declare that they have no known competing financial interests or personal relationships that could have appeared to influence the work reported in this paper.

Acknowledgments

This work was supported by the National Natural Science Foundation of China (21777094) and Ministry of Education Key Projects of Philosophy and Social Sciences Research (17JZD025).

Appendix A. Supplementary data

Supplementary data to this article can be found online at https://doi.org/10.1016/j.envpol.2020.115927.

References

Adams, M.D., 2020. Air pollution in ontario, Canada during the COVID-19 state of emergency. Sci. Total Environ. 742, 140516. https://doi.org/10.1016/j.scitotenv.2020.140516.

Ali, I., Alharbi, O.M.L., 2020. COVID-19: disease, management, treatment, and social impact. Sci. Total Environ. 728, 138861. https://doi.org/10.1016/j.scitotenv.2020.138861.

Babu, S.R., Rao, N.N., Kumar, S.V., Paul, S., Pani, S.K., 2020. Plausible role of environmental factors on COVID-19 transmission in the megacity Delhi, India. Aerosol Air Qual. Res. 20, 2075–2084. https://doi.org/10.4209/aaqr.2020.06.0314.

Bao, R., Zhang, A., 2020. Does lockdown reduce air pollution? Evidence from 44 cities in northern China. Sci. Total Environ. 731, 139052. https://doi.org/10.1016/j.scitotenv.2020.139052.

Beihai-AQM, 2020. Beihai Air Quality Monitoring. Retrieved from. http://116.11.32.203:81/.
Broomandi, P., Karaca, F., Nikfal, A., Jahanbakhshi, A., Tamjidi, M., Kim, J.R., 2020. Impact of COVID-19 event on the air quality in Iran. Aerosol Air Qual. Res. 20, 1793–1804. https://doi.org/10.4209/aaqr.2020.05.0205.
CEMS, 2020. Key Industrial Sources Emissions. Retrieved from. http://202.103.233.156:7311/.
Chen, L., Zhu, J., Liao, H., Yang, Y., Yue, X., 2020. Meteorological influences on $PM_{2.5}$ and O_3 trends and associated health burden since China's clean air actions. Sci. Total Environ. 744, 140837. https://doi.org/10.1016/j.scitotenv.2020.140837.
ERA-Interim, 2020. Medium-Range Weather Forecasts Reanalysis Interim. Retrieved from. https://apps.ecmwf.int/datasets/.
Fu, S., Guo, M., Luo, J., Han, D., Chen, X., Jia, H., Jin, X., Liao, H., Wang, X., Fan, L., Cheng, J., 2020. Improving VOCs control strategies based on source characteristics and chemical reactivity in a typical coastal city of South China through measurement and emission inventory. Sci. Total Environ. 744, 140825. https://doi.org/10.1016/j.scitotenv.2020.140825.
Hong, Z., Li, M., Wang, H., Xu, L., Hong, Y., Chen, J., Chen, J., Zhang, H., Zhang, Y., Wu, X., Hu, B., Li, M., 2019. Characteristics of atmospheric volatile organic compounds (VOCs) at a mountainous forest site and two urban sites in the southeast of China. Sci. Total Environ. 657, 1491–1500. https://doi.org/10.1016/j.scitotenv.2018.12.132.
Hui, L., Liu, X., Tan, Q., Feng, M., An, J., Qu, Y., Zhang, Y., Jiang, M., 2018. Characteristics, source apportionment and contribution of VOCs to ozone formation in Wuhan, Central China. Atmos. Environ. 192, 55–71. https://doi.org/10.1016/j.atmosenv.2018.08.042.
Hui, L., Liu, X., Tan, Q., Feng, M., An, J., Qu, Y., Zhang, Y., Cheng, N., 2019. VOC characteristics, sources and contributions to SOA formation during haze events in Wuhan, Central China. Sci. Total Environ. 650, 2624–2639. https://doi.org/10.1016/j.scitotenv.2018.10.029.
Kuerban, M., Waili, Y., Fan, F., Liu, Y., Qin, W., Dore, A.J., Peng, J., Xu, W., Zhang, F., 2020. Spatio-temporal patterns of air pollution in China from 2015 to 2018 and implications for health risks. Environ. Pollut. 258, 113659. https://doi.org/10.1016/j.envpol.2019.113659.
Li, L., Li, Q., Huang, L., Wang, Q., Zhu, A., Xu, J., Liu, Z., Li, H., Shi, L., Li, R., Azari, M., Wang, Y., Zhang, X., Liu, Z., Zhu, Y., Zhang, K., Xue, S., Ooi, M., Zhang, D., Chan, A., 2020. Air quality changes during the COVID-19 lockdown over the Yangtze River Delta Region: an insight into the impact of human activity pattern changes on air pollution variation. Sci. Total Environ. 732, 139282. https://doi.org/10.1016/j.scitotenv.2020.139282.
Liao, T., Wang, S., Ai, J., Gui, K., Duan, B., Zhao, Q., Zhang, X., Jiang, W., Sun, Y., 2017. Heavy pollution episodes, transport pathways and potential sources of $PM_{2.5}$ during the winter of 2013 in Chengdu (China). Sci. Total Environ. 584 (585), 1056–1065. https://doi.org/10.1016/j.scitotenv.2017.01.160.
Liu, Y., Wang, T., 2020. Worsening urban ozone pollution in China from 2013 to 2017-part1: the complex and varying roles of meteorology. Atmos. Chem. Phys. Discuss. https://doi.org/10.5194/acp-2019-1120.
Liu, H., Chen, Z., Mo, Z., Li, H., Huang, J., Liang, G., Yang, J., Yang, J., Zhang, D., Chen, X., Yang, J., 2019. Emission inventory of atmospheric pollutants from industrial sources and its spatial characteristics in Guangxi. Acta Sci. Circumstantiae 39, 229–242. https://doi.org/10.13671/j.hjkxxb.2018.0366 (in Chinese).
Liu, Q., Sha, D., Liu, W., Houser, P., Zhang, L., Hou, R., Lan, H., Flynn, C., Lu, M., Hu, T., Yang, C., 2020. Spatiotemporal patterns of COVID-19 impact on human activities and environment in mainland China using nighttime light and air quality data. Rem. Sens. 12, 1576. https://doi.org/10.3390/rs12101576.
MEE, 2020. The Air Monitoring Data Center. Retrieved from. http://datacenter.mep.gov.cn.
Monks, P.S., Archibald, A.T., Colette, A., Cooper, O., Coyle, M., Derwent, R., Fowler, D., Granier, C., Law, K.S., Mills, G.E., Stevenson, D.S., Tarasova, O., Thouret, V., Schneidemesser, E. von, Sommariva, R., Wild, O., Williams, M.L., 2015. Tropospheric ozone and its precursors from the urban to the global scale from air quality to short-lived climate forcer. Atmos. Chem. Phys. 15, 8889–8973. https://doi.org/10.5194/acp-15-8889-2015.
Pei, Z., Han, G., Ma, X., Su, H., Gong, W., 2020. Response of major air pollutants to COVID-19 lockdowns in China. Sci. Total Environ. 743, 140879. https://doi.org/10.1016/j.scitotenv.2020.140879.
Qu, Y., An, J., He, Y., Zheng, J., 2016. An overview of emissions of SO_2 and NOx and the long-range transport of oxidized sulfur and nitrogen pollutants in East Asia. J. Environ. Sci. 44, 13–25. https://doi.org/10.1016/j.jes.2015.08.028.
Rolph, G., Stein, A., Stunder, B., 2017. Real-time environmental applications and display sYstem: ready. Environ. Model. Software 95, 210–228. https://doi.org/10.1016/j.envsoft.2017.06.025.
Sharma, S., Zhang, M., Anshika Gao, J., Zhang, H., Kota, S.H., 2020. Effect of restricted emissions during COVID-19 on air quality in India. Sci. Total Environ. 728, 138878. https://doi.org/10.1016/j.scitotenv.2020.138878.
Shen, L., Mickley, L.J., Murray, L.T., 2017. Influence of 2000–2050 climate change on particulate matter in the United States: results from a new statistical model. Atmos. Chem. Phys. 17, 4355–4367. https://doi.org/10.5194/acp-17-4355-2017.
Shu, L., Xie, M., Gao, D., Wang, T., Fang, D., Liu, Q., Huang, A., Peng, L., 2017. Regional severe particle pollution and its association with synoptic weather patterns in the Yangtze River Delta region, China. Atmos. Chem. Phys. 17, 1–31. https://doi.org/10.5194/acp-2017-473.
Sicard, P., De Marco, A., Agathokleous, E., Feng, Z., Xu, X., Paoletti, E., Rodriguez, J.J.D., Calatayud, V., 2020. Amplified ozone pollution in cities during the COVID-19 lockdown. Sci. Total Environ. 735, 139542. https://doi.org/10.1016/j.scitotenv.2020.139542.
Siciliano, B., Dantas, G., da Silva, C.M., Arbilla, G., 2020. Increased ozone levels during the COVID-19 lockdown: analysis for the city of Rio de Janeiro, Brazil. Sci. Total Environ. 737, 139765. https://doi.org/10.1016/j.scitotenv.2020.139765.
Sun, L., Xue, L., Wang, T., Gao, J., Ding, A., Cooper, O.R., Lin, M., Xu, P., Wang, Z., Wang, X., Wen, L., Zhu, Y., Chen, T., Yang, L., Wang, Y., Chen, J., Wang, W., 2016. Significant increase of summertime ozone at mount tai in central eastern China. Atmos. Chem. Phys. 16, 10637–10650. https://doi.org/10.5194/acp-16-10637-2016.
Sun, Y., Lei, L., Zhou, W., Chen, C., He, Y., Sun, J., Li, Z., Xu, W., Wang, Q., Ji, D., Fu, P., Wang, Z., Worsnop, D.R., 2020. A chemical cocktail during the COVID-19 outbreak in Beijing, China: insights from six-year aerosol particle composition measurements during the Chinese New Year holiday. Sci. Total Environ. 742, 140739. https://doi.org/10.1016/j.scitotenv.2020.140739.
Tang, L., Li, Y., Deng, X., Johnston, N.J., Liu, G., Liu, S., 2013. Characteristics of water-soluble anion in atmospheric in northern suburb of Nanjing in winter. Trans. Atoms. Sci. 36, 489–498. http://www.biomedcentral.com/1471-2164/14/489.
Wang, T., Xue, L., Brimblecombe, P., Lam, Y.F., Li, L., Zhang, L., 2017. Ozone pollution in China: a review of concentrations, meteorological influences, chemical precursors, and effects. Sci. Total Environ. 575, 1582–1596. https://doi.org/10.1016/j.scitotenv.2016.10.081.
Wang, J., Yang, Y., Zhang, Y., Niu, T., Jiang, X., Wang, Y., Che, H., 2019. Influence of meteorological conditions on explosive increase in O_3 concentration in troposphere. Sci. Total Environ. 652, 1228–1241. https://doi.org/10.1016/j.scitotenv.2018.10.228.
Yang, C., Sha, D., Liu, Q., Li, Y., Lan, H., Guan, W.W., Hu, T., Li, Z., Zhang, Z., Thompson, J.H., Wang, Z., Wong, D., Ruan, S., Yu, M., Richardson, D., Zhang, L., Hou, R., Zhou, Y., Zhong, C., Tian, Y., Beaini, F., Carte, K., Flynn, C., Liu, W., Pfoser, D., Bao, S., Li, M., Zhang, H., Liu, C., Jiang, J., Du, S., Zhao, L., Lu, M., Li, L., Zhou, H., Ding, A., 2020. Taking the pulse of COVID-19: a spatiotemporal perspective. International journal of digital earth 1–26. https://doi.org/10.1080/17538947.2020.1809723.
Zhai, S., Jacob, D.J., Wang, X., Shen, L., Li, K., Zhang, Y., Gui, K., Zhao, T., Liao, H., 2019. Fine particulate matter ($PM_{2.5}$) trends in China, 2013–2018: separating contributions from anthropogenic emissions and meteorology. Atmos. Chem. Phys. 19, 11031–11041. https://doi.org/10.5194/acp-19-11031-2019.
Zhang, Y.L., Cao, F., 2015. Fine particulate matter ($PM_{2.5}$) in China at a city level. Sci. Rep. 5, 14884. https://doi.org/10.1038/srep14884.
Zhang, Y., Ding, A., Mao, H., Nie, W., Zhou, D., Liu, L., Huang, X., Fu, C., 2016. Impact of synoptic weather patterns and inter-decadal climate variability on air quality in the North China Plain during 1980–2013. Atmos. Environ. 124, 119–128. https://doi.org/10.1016/j.atmosenv.2015.05.063.
Zhang, Y., West, J.J., Mathur, R., Xing, J., Hogrefe, C., Roselle, S.J., Bash, J.O., Pleim, J.E., Gan, C.M., Wong, D.C., 2018. Long-term trends in the ambient $PM_{2.5}$- and O_3-related mortality burdens in the United States under emission reductions from 1990 to 2010. Atmos. Chem. Phys. 18, 15003–15016. https://doi.org/10.5194/acp-18-15003-2018.
Zhang, L., An, J., Liu, M., Li, Z., Liu, Y., Tao, L., Liu, X., Zhang, F., Zheng, D., Gao, Q., Guo, X., Luo, Y., 2020a. Spatiotemporal variations and influencing factors of $PM_{2.5}$ concentrations in Beijing, China. Environ. Pollut. 262, 114276. https://doi.org/10.1016/j.envpol.2020.114276.
Zhang, Z., Xue, T., Jin, X., 2020b. Effects of meteorological conditions and air pollution on COVID-19 transmission: evidence from 219 Chinese cities. Sci. Total Environ. 741, 140244. https://doi.org/10.1016/j.scitotenv.2020.140244.
Zhao, S., Yin, D., Yu, Y., Kang, S., Qin, D., Dong, L., 2020. $PM_{2.5}$ and O_3 pollution during 2015–2019 over 367 Chinese cities: spatiotemporal variations, meteorological and topographical impacts. Environ. Pollut. 264, 114694. https://doi.org/10.1016/j.envpol.2020.114694.
Zheng, B., Tong, D., Li, M., Liu, F., Hong, C., Geng, G., Li, H., Li, X., Peng, L., Qi, J., Yan, L., Zhang, Y., Zhao, H., Zheng, Y., He, K., Zhang, Q., 2018. Trends in China's anthropogenic emissions since 2010 as the consequence of clean air actions. Atmos. Chem. Phys. 18, 14095–14111. https://doi.org/10.5194/acp-2018-374.
Zheng, H., Kong, S., Chen, N., Yan, Y., Liu, D., Zhu, B., Xu, K., Cao, W., Ding, Q., Lan, B., Zhang, Z., Zheng, M., Fan, Z., Cheng, Y., Zheng, S., Yao, L., Bai, Y., Zhao, T., Qi, S., 2020. Significant changes in the chemical compositions and sources of $PM_{2.5}$ in Wuhan since the city lockdown as COVID-19. Sci. Total Environ. 739, 140000. https://doi.org/10.1016/j.scitotenv.2020.140000.
Zhu, J., Chen, L., Liao, H., Dang, R., 2019. Correlations between $PM_{2.5}$ and ozone over China and associated underlying reasons. Atmosphere 10. https://doi.org/10.3390/atmos10070352.